Volume 16
Number 10
21 May 2025
Pages 3741-4190

Food & Function

Linking the chemistry and physics of food with health and nutrition

rsc.li/food-function

ISSN 2042-650X

ROYAL SOCIETY OF CHEMISTRY

PAPER

Feitong Liu, Bin Zhang *et al.*
Bifidobacterium breve HH079 alleviates early-life antibiotic-exposed colon dysbiosis in mice by restoring the gut microbiota and gut barrier function

Food & Function

ROYAL SOCIETY OF CHEMISTRY

PAPER

View Article Online
View Journal | View Issue

Cite this: *Food Funct.*, 2025, **16**, 3833

Bifidobacterium breve HH079 alleviates early-life antibiotic-exposed colon dysbiosis in mice by restoring the gut microbiota and gut barrier function†

Zhipeng Gu,[a] Zerong Lu,[b] Jian-yong Wu,[c] Zhuqing Xie,[a] Ruibiao Hu,[b] Qiang Huang,[a] Feitong Liu*[b] and Bin Zhang*[a,d]

Antibiotic exposure in early life disrupts gut microbiota development in infants, which could result in intestinal dysfunction. This study mimicked early-life antibiotic exposure in mice by administering antibiotic water to lactating dams, and investigated the effects of a new strain of *Bifidobacterium breve* HH079 (*B. breve* HH079) on intestinal dysbiosis associated with early-life antibiotic exposure in pups. The results showed that *B. breve* HH079 treatment inhibited the proliferation of *Pseudomonas* and *Morganella* after antibiotic exposure, but promoted the abundance of *Bifidobacterium* and *Bacteroides* and acetate production. Concomitantly, the *B. breve* HH079 administration resulted in decreased M1 gene (*Cd86*) and protein (TNF-α, IL-1β, LBP and iNOS) expression and increased M2 macrophage marker (*Cd206*, IL-10 and Arg1) expression in the colonic macrophages of antibiotic-exposed pups, probably by inhibiting the TLR4/NF-κB pathway. Moreover, there was increased intestinal epithelial tight junction protein (Cldn1 and Ocln) expression and the transcription of marker gene (*Lyz2*, *Igha* and *Reg3β*) normalization involved in innate immunity. The results suggested that the new *B. breve* HH079 strain could alleviate early-life antibiotic-induced colon dysbiosis by regulating the gut microbiota and promoting acetate production and the subsequent M2 macrophage polarization to recover gut health.

Received 27th January 2025,
Accepted 8th March 2025

DOI: 10.1039/d5fo00535c

rsc.li/food-function

Introduction

Although breast milk is an excellent source of nutrition and the perfect food for babies, antibiotics are often detected in the breast milk of lactating mothers, even for those who have not been offered antibiotics during pregnancy and lactation.[1] Antibiotics in the maternal circulation could enter breast milk through passive diffusion, increasing the risk of antibiotic exposure in infants.[2,3] Continued exposure to antibiotics delays gut microbiota maturation and disturbs the immune environment balance in early life, which in turn affects long-term health outcomes, including increased susceptibility to diseases such as obesity, allergies, gastrointestinal diseases and infections.[4,5] A prospective cohort study has shown that intrapartum antibiotic exposure reduced the abundance of the immune modulation-related microbiota (*e.g.*, *Bacteroides* and *Bifidobacterium*) at one year of age, compared to infants without exposure.[6] Early-life antibiotic treatment has been shown with the disruptive development of intestinal Peyer's patches, overactive intestinal macrophages, and even shortened host longevity in mouse models.[7,8] Maternal antibiotic treatment also has significant and persistent effects on antibiotic resistance genes in the infant gut, providing favorable conditions for the colonization of *E. coli* and Gammaproteobacteria, thereby accelerating the development of antibiotic-resistant infections.[9,10]

Four infant gut microbiota-dominant enterotypes, including Firmicutes, *Bifidobacterium*, *Bacteroides*, and *Prevotella*, have been identified by the metagenomic sequencing analysis of 13 776 fecal samples from 1956 infants in 17 countries.[11] *Bifidobacteria* are among the pivotal gastrointestinal colonizers during the first six months of infants, and have been adopted as novel live biotherapeutics to restore the microbiota composition for infant health.[4] In a Japanese cohort study, Horigome *et al.* reported that *Bifidobacterium breve* (*B. breve*) adminis-

[a]*School of Food Science and Engineering, Overseas Expertise Introduction Center for Discipline Innovation of Food Nutrition and Human Health, South China University of Technology, Guangzhou 510640, China. E-mail: zhangb@scut.edu.cn*
[b]*H&H Group, H&H Research, Global Research and Technology Center, Guangzhou 510700, China. E-mail: erin.liu@hh.global*
[c]*Research Institute for Future Food, Department of Applied Biology and Chemical Technology, The Hong Kong Polytechnic University, Hung Hom, Kowloon, Hong Kong, China*
[d]*Sino-Singapore International Research Institute, Guangzhou 510555, China*
† Electronic supplementary information (ESI) available. See DOI: https://doi.org/10.1039/d5fo00535c

tration increased the colonization time at least three weeks longer in the intestines of low-birth-weight (LBW) infants (n = 12) compared with the control group (LBW infants without probiotic supplementation, n = 10).[12] Antibiotic-induced gut microbiota dysbiosis accelerates the translocation of LPS and other immunogenic bacterial compounds, leading to overpolarization of intestinal macrophages and impaired intestinal stem cell differentiation.[13] In a double-blind randomized trial, Sanyang *et al.* analyzed the fecal samples of 127 infants in Gambia at the age of 1 month by 16S rRNA sequencing, and found that intrapartum antibiotic exposure destroyed the composition of the gut microbiota, including promoting Enterobacteriaceae and Enterococcaceae, reducing the abundance of *Bifidobacterium*.[14] In a double-blind trial study, Korpela *et al.* analyzed the fecal samples from 428 infants in Helsinki at the age of 3 months by 16S rRNA sequencing, and found that continued supplementation of probiotic mixtures (containing *B. breve*) in early life prevented or corrected the antibiotic treatment-induced increase in Bacteroidaceae, Enterococcaceae and Enterobacteriaceae and decline in Bifidobacteriaceae.[15] Additionally, the *Bifidobacteria* fermentation metabolites, *i.e.*, short-chain fatty acids (SCFAs), particularly acetate, can affect the phenotype and function of macrophages by activating G protein-coupled receptors (GPCRs), blocking pro-inflammatory responses after pathogen and LPS stimulation, and thus regulate intestinal permeability.[16,17] In a pilot trial, Alba *et al.* analyzed the fecal samples from 160 infants in Madrid at the age of 6 months, and found that infants receiving *B. breve* supplementation for 90 days exhibited increased fecal levels of *Bifidobacterium* and SCFAs, as well as significant reductions in gastrointestinal and respiratory tract infection rates.[18] Although *B. breve* is well documented for its beneficial effect on the restoration and prevention of gastrointestinal microbiota dysbiosis in infants, its role in intestinal barrier integrity and immune function under early-life antibiotic exposure remains unclear.

To address this topic, we modeled antibiotic exposure in neonatal mice by administering antibiotic water to lactating dams, and evaluated the regulatory effects of a new *B. breve* strain, *B. breve* HH079, on gut ecology in pups impaired by antibiotic exposure. We determined the effects of *B. breve* HH079 supplementation on the gut microbiota community structure, as well as the modulatory effects on the colonic macrophage phenotype and gut barrier function. It is expected that the present study may advance the understanding of *B. breve* as a potential live biotherapeutic during periods of infant microbiota vulnerability caused by antibiotic exposure.

Materials and methods

Experimental strains

Bifidobacterium breve HH079 was sourced from the Global Research and Technology Center, H&H Group. (Guangzhou, China). According to our previous method,[19] the strain was incubated anaerobically in an MRS medium at 37 °C, followed by two subcultures under the same conditions. The bacterial precipitation was collected by centrifugation at 8000g for 15 min, and then resuspended in PBS.

Mice

Specific pathogen-free (SPF) C57BL/6J pregnant mice (8–10 weeks, first gestation) were purchased from Hunan SJA Laboratory Animal Co., Ltd (Changsha, China). These mice were placed in a controlled environment with a temperature ranging from 22 ± 2 °C, a humidity ranging from 52 ± 3%, and a 12 h light/dark cycle. The pregnant dams were individually housed, and provided with an AIN-93G standard diet and *ad libitum* access to drinking water. The experimental procedure was approved by the Ethics Committee of the Guangdong Academy of Sciences (approval no. K202401021).

Antibiotic treatment and *B. breve* HH079 administration

A mouse model of early-life gut microbiota dysbiosis induced by antibiotic exposure was established as previously described.[20] An antibiotic cocktail of 1 g L^{-1} ampicillin (Sigma, Darmstadt, Germany) and 0.5 g L^{-1} neomycin (Sigma, Darmstadt, Germany) was delivered *via* drinking water to the designated lactating dams from day 1 to day 21 postpartum. The offspring received antibiotic challenges through breast-feeding on postnatal day 1 (P1) until weaning (postnatal day, P21). All drinking water was filter sterilized before administration, and antibiotic water was refreshed every two days.

In the *B. breve* HH079 intervention experiment, pups were randomly allocated to 3 groups (n = 7–9 offspring from 2–3 litters per group): (i) received maternal milk from non-antibiotic-treated dams (Con group); (ii) received maternal milk from antibiotic-treated dams (Abx group); and (iii) received maternal milk from antibiotic-treated dams in conjunction with *B. breve* HH079 suspension gavage (HH079 group). During the period of 10 to 21 days of birth, pups in the Con and Abx groups received PBS daily, and the HH079 group was administered with the bacterial suspension (10^9 CFU mL^{-1} of *B. breve* HH079 in PBS) daily. Fresh pup feces were collected prior to sacrifice and stored at −80 °C. The pups were humanely euthanized by CO_2 asphyxiation. The colon, serum and colon contents from pups were also collected and stored at −80 °C until analysis.

Histology, immunohistochemistry and immunofluorescence

The mouse colon tissues were routinely histopathologically processed and stained as previously described.[13] Briefly, the colon tissue was fixed in 4% paraformaldehyde for 24 h, and then embedded in paraffin blocks. The tissue samples were then divided into 4 μm slices. The slices were de-waxed in xylene, rehydrated through graded alcohols, and stained with hematoxylin–eosin (H&E) or alcian blue/periodic acid-Schiff (AB/PAS) for histological examination. Coverslips were then fixed by using Cytoseal 60 (83114, Thermo Fisher Scientific, USA), and imaged using a light microscope (BX 53M, Olympus, Japan). The H&E-stained samples were scored to evaluate the extent of tissue damage, as previously described.[21]

For IHC-paraffin sections, the paraffin-embedded sections were washed with citrate buffer for antigen unmasking. These slices were blocked with 10% bovine serum albumin (BSA), and then incubated with a MUC2 antibody (1 : 1800, GB11344, Servicebio) at 4 °C overnight. After washing, the sections were incubated with a HRP-conjugated secondary antibody (1 : 500, GB23303, Servicebio) for 1 h and stained with a DAB Substrate Kit (8059, CST, USA). For IF-Paraffin sections, anti-arginase 1 (1 : 500, GB11285, Servicebio) and anti-iNOS (1 : 1000, GB11119, Servicebio) antibodies were incubated at 4 °C overnight. Following primary antibody incubation, the sections were washed and incubated with Alexa Fluor 488-conjugated goat anti-rabbit IgG (1 : 500, GB25301, Servicebio). The sections were then stained with DAPI (ab104139, Abcam) for nuclear visualization and examined using a Leica DMi8 fluorescence microscope (Leica, DMi8, Germany). Subsequently, the fluorescence intensity was quantified by using ImageJ software (v.1.52, NIH, USA).

ELISA

The concentrations of IL-1β, TNF-α, IL-10, and LBP in the offspring serum were measured according to the manufacturer's instructions of the mouse-derived specific ELISA kit (Xinyu, Shanghai, China). Briefly, the diluted cytokine standard and offspring serum (10 μL) were added to the 96-well plate and incubated at 37 °C for 1 h. Subsequently, the horseradish peroxidase (HRP) secondary antibody (100 μL) was added, and incubated at 37 °C for 30 min to label the target proteins. After washing five times with TBST, the sample wells were incubated with TMB chromogen solution (100 μL) for 15 min at 37 °C. After the reaction was terminated by adding the stop solution, the optical density (OD) at 450 nm of each well was measured immediately using a Spark Cyto System (Tecan, Switzerland), and the concentration of the target cytokines in the samples was calculated by plotting the standard curve.

Real-time quantitative PCR (RT-qPCR)

Total RNA was extracted from the colonic tissues using the Total RNA Extraction Kit (Promega). RNA purity and concentration were assessed using a NanoDrop spectrophotometer (Thermo Fisher), based on the absorbance at 260 and 280 nm. The purified RNA was used to synthesize cDNA using the RevertAid RT Kit (K1691, Thermo Fisher Scientific, USA) following the protocols. The primer sequences for the target genes used in the study (Table S1†) were obtained from PrimerBank. SYBR Premix Ex Taq (Vazyme, Nanjing) was used to perform the quantitative PCR by using the real-time fluorescent Quantitative PCR System (CFX384 Touch, BioRad, USA). Each gene cycle threshold (Ct) was analyzed and normalized to the GAPDH reference gene.

Flow cytometry analysis

Flow cytometry analysis was performed using the mouse colon tissue according to the method previously described.[22] Briefly, colon tissues were minced and incubated in Hank's balanced salt solution (H8264, Sigma, Germany) supplemented with 5 mM EDTA and DTT for 30 min to isolate the intestinal epithelial cells. The intestinal pieces were digested in an RPMI medium containing 1% collagenase I and 10% trypsin for 30 min under shaking conditions to isolate the lamina propria cells. The resulting cell suspensions were harvested *via* a 70-μm cell filter and preserved in an FACS buffer. Colon lamina propria cells were labeled with the following antibodies: anti-mouse CD45 (557659, BD Pharmingen), anti-mouse CD3e (553062, BD Pharmingen), anti-CD11b (553312, BD Pharmingen) and anti-mouse F4/80 (565411, BD Pharmingen). Flow samples were determined using a flow cytometry system (BD FACS Celesta, USA), and data were processed using FlowJo software (v10.6.2, USA).

Protein extraction and western blotting (WB)

Total protein from the colon tissue samples was extracted with RIPA buffer containing PMSF inhibitors (NCM Biotech, China) according to our previous method,[23] and its concentration was determined using the BCA protein assay kit (Beyotime, China). Tissue proteins were separated by 4–20% SDS-PAGE and then combined with 0.45 μm polyvinylidene fluoride (PVDF) membranes. The PVDF membranes were blocked with 5% skim milk for 2 h and incubated overnight at 4 °C with primary antibodies, including occludin (1 : 1000, ab216327, Abcam), MyD88 (1 : 1000, ab219413, Abcam), IκB α (1 : 1000, ab32518, Abcam), NF-κB p65 (1 : 1000, ab16502, Abcam), GAPDH (1 : 1000, 5174, CST) and FFAR2 (1 : 1000, 19952, Proteintech). After washing five times with TBST, the membranes were incubated with secondary antibodies for 1 h at room temperature. The protein bands were imaged in the Gel Doc XR+ System (Bio-Rad, USA) using a chemiluminescence kit (Biosharp, China). Ultimately, the protein bands were densitometrically quantified using ImageJ software and normalized to the GAPDH expression in each sample.

16S rRNA sequencing and bioinformatics

The 16S rRNA amplicon sequencing was performed as described previously with slight modifications.[24] The total microbial DNA was extracted from the mouse feces using a QIAamp DNA Mini-Kit (Qiagen, Hilden, Germany). The V3–V4 region of the 16S rRNA gene was amplified for each sample using primer pairs 338F (5′-ACTCCTACGGGGGAGGCAGCA-3′) and 806R (5′-GGACTACHVGGGGTWTCTAAT-3′). The PCR products were purified using Ampure magnetic purification beads (Beckman, USA) and then sequenced on an Illumina MiSeq sequencer (Illumina, USA) at Shanghai Personal Biotechnology Co., Ltd. Amplicon sequence variants (ASVs) were generated by filtering the raw sequence through QIIME2 DADA2.[25] Alpha-diversity indices were assessed based on the *Alpha_diversity.py* command line. The principal coordinate analysis (PCoA) and the analysis of ADONIS using the Bray–Curtis distance matrix were used to detect the microbial community changes between the experimental groups. Dissimilarities among the treatment groups were examined by LEfSe.

Short-chain fatty acid (SCFA) determination

The SCFA concentration in the mouse colon content was quantified following the method used in a previous study.[26,27] Briefly, colonic contents (40 mg) were mixed with 200 μL of 15% metaphosphoric acid containing 50 mM 4-methyl-pentanoic acid (as the internal standard). The mixture was ground and then centrifuged at 12 000 rpm for 10 min to collect the supernatant. SCFAs in the supernatant were identified and quantified by gas chromatography with flame ionization detection (GC-FID, Agilent, CA). For the chromatographic process, samples (0.2 μL) were separated on a polar ZB-FFAP column (30 m × 0.25 mm × 0.25 mm) with a constant nitrogen flow rate of 1 mL min^{-1}. The flame ionization detector and injection port were maintained at 250 °C and 280 °C, respectively. SCFA concentrations were determined by comparing the relative peak areas of the target compounds to the internal standard.

Transcriptomic analysis

Total RNA was extracted from the colon tissue by using the TRIzol reagent (Sangon, Shanghai, China) and the RNA integrity was determined by using an 2100 Expert bioanalyzer (Agilent, USA). Transcriptome sequencing libraries were generated on an Illumina NovaSeq platform according to the manufacturer's (Wekemo, Shenzhen, China) protocol. Clean transcript content was constructed by using featureCounts software by removing splices and low-quality reads from the raw data.[28] The gene expression of transcripts was corrected using the edgeR package.[29] Differentially expressed genes (DEGs) were identified based on the criteria of $|\log_2(\text{FoldChange})| > 1$ and p-adjust <0.05. The DEGs were visualized using a heat map to display the expression patterns. The Kyoto Encyclopedia of Genes and Genomes (KEGG) enrichment analysis was conducted using the ClusterProfiler package to achieve the functional annotation of the transcripts.[30]

Statistical analysis

One-way analysis of variance (ANOVA) was performed on the data from the different groups, and a *post hoc* Tukey test was conducted to determine the significant differences. Correlation analyses were based on Pearson's correlation analysis. Data were expressed as mean ± standard deviation (SD). $P < 0.05$ was considered to be statistically significant. The figures were plotted using GraphPad Prism 8.0 (CA, USA) or R (Vienna, Austria).

Results

B. breve HH079 promotes body growth and colon development in early-life antibiotic-exposed pups

To investigate the effect of *B. breve* HH079 supplementation on gut development in early-life antibiotic-exposed mice, we established a mouse model in which dams were continuously provided with antibiotic water during lactation, and the pups were treated with *B. breve* HH079 administration from P10 until weaning. In this model, the neonatal mouse gut microbiome was challenged by ampicillin and neomycin during breastfeeding. Neomycin is effective against most Gram-negative bacteria, and ampicillin is mostly used as a broad-spectrum antibiotic for newborns against Gram-positive and Gram-negative bacteria.[31] We first investigated the influence of *B. breve* HH079 administration on body growth and colon development following early-life antibiotic exposure. It was noted that antibiotics did not affect the total food intake of dams in all treatment groups (Fig. 1B), but significantly reduce pup weight compared to the Con group (Fig. 1C). *B. breve* HH079 supplementation reversed the weight loss caused by antibiotic exposure and reached the level corresponding to the Con group. We also observed a significant increase in the colon length in the HH079 group compared to the Abx group (Fig. 1D and E). Colon histology also showed significantly increased colonic histopathology scores induced by early-life antibiotic exposure, including mild inflammatory infiltrates, crypt irregularities, and goblet cell loss (Fig. 1F and G). *B. breve* HH079 supplementation significantly inhibited inflammatory cell infiltration and increased the number of colonic GCs and considerably reduced the histological score (Fig. 1F and G).

B. breve HH079 regulates the gut microbial communities in early-life antibiotic-exposed pups

The effect of *B. breve* HH079 supplementation on the fecal microbiota of pups following early-life antibiotic exposure was evaluated. Measurements of the observed species, Chao1, Shannon and Simpson indexes suggested a significant reduction in fecal microbiota richness and evenness in the Abx group pups (Fig. 2B). Interestingly, the reduced alpha diversity in the Abx group was reversed by *B. breve* HH079 supplementation, indicating that *B. breve* HH079 significantly affected gut microbial diversity in pups. Weighted UniFrac dissimilarity-based PCoA analysis further showed evident groupings of the microbiota in the Con, Abx and HH079 groups, and the HH079 group clustering closer to the control pups than the Abx group (Fig. 2C; ADONIS $R^2 = 0.95$ and $p = 0.001$), suggesting that *B. breve* HH079 supplementation during antibiotic exposure steered microbiome recovery toward a more consistent community structure.

We also compared the taxon-specific abundance of gut microbes between the treatment groups. Here, only 25 identical ASVs were shared among the Con, Abx, and HH079 groups (Fig. 2A), suggesting that early-life antibiotic exposure altered the gut microbiota profile of the pups. At the phylum level, early-life antibiotic exposure significantly reduced the abundance of Bacteroidetes and promoted Proteobacteria in the gut microbiota of pups compared to the Con group, whereas *B. breve* HH079 supplementation significantly enriched Bacteroidetes and Actinobacteria, and inhibited the relative abundance of Proteobacteria (Fig. 2D). Specifically, *Prevotella* and *Parabacteroides* as enriched colonies in the Con group dominated in the taxonomic composition (Fig. 2E and F). The microbiota showed a significant shift towards a community dominated by *Pseudomonas*, *Enterococcus*, *Paenibacillus* and *Morganella* in the Abx group (Fig. 2E and Fig. S1†), indicating that the gut microbiota of pups were severely disturbed by antibiotic exposure.[32] In contrast, pups supplemented with

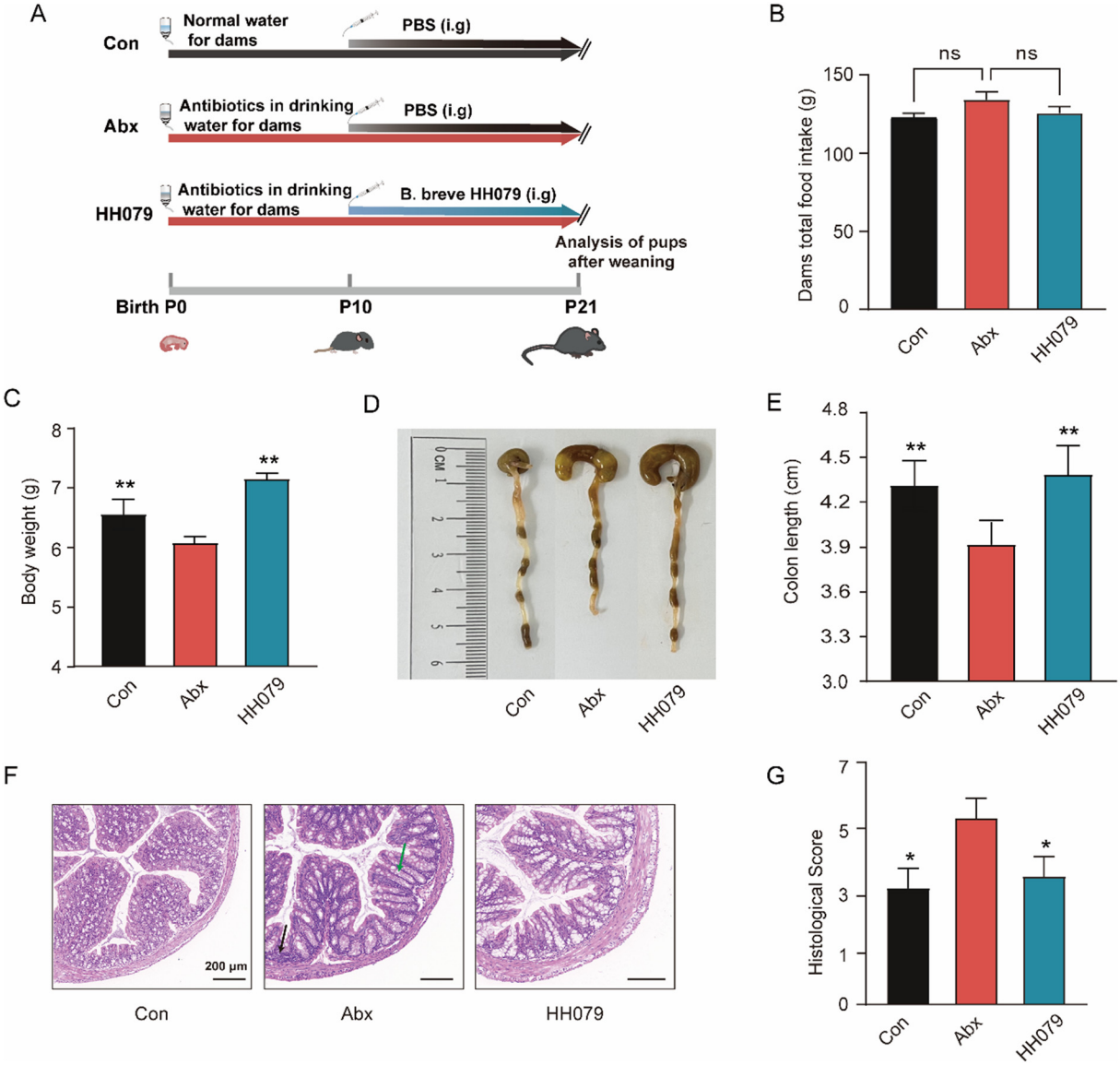

Fig. 1 Effect of *B. breve* HH079 administration on the body growth and colon development in early-life antibiotic-exposed mice. (A) Experimental design of antibiotic exposure and *B. breve* HH079 administration in the early life of mice. (B) Total food intake of dams. (C) Body weight of pups on P21. (D) Representative macroscopic pictures of colons from the different groups. (E) Colon length. (F) Representative images of H&E staining (black arrow – inflammatory infiltrates; green arrow – goblet cells) and (G) Histological score of the colon. *$P < 0.05$ and **$P < 0.01$ indicated significant differences compared to the Abx group.

B. breve HH079 during exposure to antibiotics refilled the microbial ecological niches after the treatment, wherein *Bifidobacterium* and *Bacteroides* were the most prominent members (Fig. 2E and F). These results demonstrated that early-life *B. breve* HH079 supplementation was an effective treatment for reshaping the gut microbiota diversity and composition disrupted by antibiotic exposure.

B. breve HH079 repairs the intestinal barrier in early-life antibiotic-exposed pups

We investigated the effects of *B. breve* HH079 on colonic epithelial injury induced by early-life antibiotic exposure in pups. Colonic goblet cells (GCs) are the major producers and synthesizers of mucus proteins, and their depletion is characteristic of intestinal barrier damage.[33] AB/PAS staining revealed a marked decrease in colon GC numbers following the early-life antibiotic exposure, while *B. breve* HH079 administration prevented the loss of the colonic mucus-producing cells (Fig. 3A and C). The loss of GCs in the mucus layer of antibiotic-exposed pups resulted in a significantly reduced MUC2 protein expression compared to the Con group (Fig. 3B and D). Tight junctions (TJs) are an important structural basis for maintaining the junction of intestinal epithelial cells.[34] Early-life antibiotic exposure significantly down-regulated *ZO-1* and *Cldn1* gene expression (Fig. 3E and G), implying that early-life gut microbiota dysbiosis disrupts epithelial cell barrier integrity

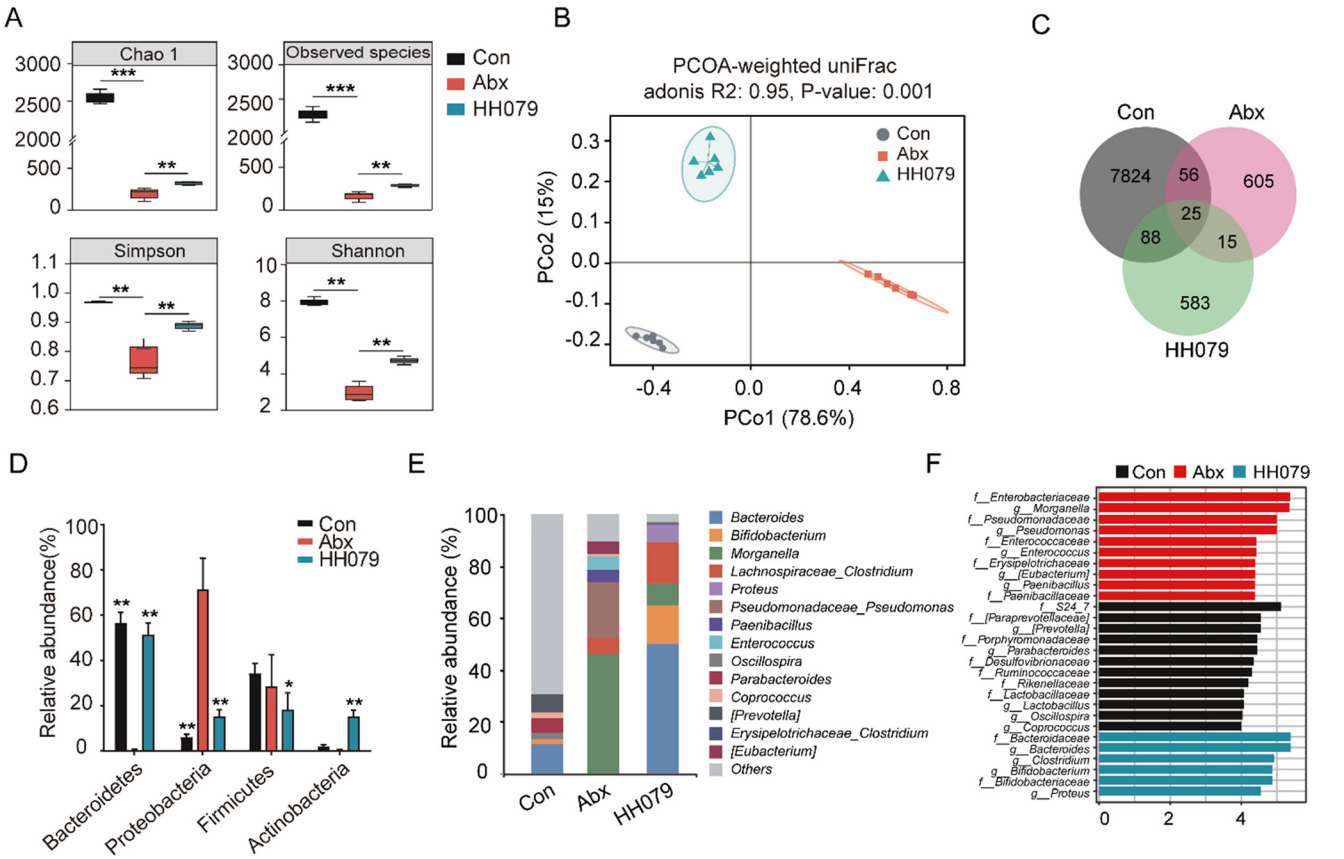

Fig. 2 *B. breve* HH079 regulates the microbiome communities in early-life antibiotic-exposed pups. (A) Alpha-diversity indices (Chao 1, observed species, Simpson, and Shannon) are shown in the boxplot. (B) Beta-diversity dissimilarity matrix was assessed through PCoA analysis. Each dot represents an individual sample. (C) Venn analysis showed common and different ASVs in all groups. (D) Relative abundance of the gut microbiota at the phylum level. (E) Relative abundance of the gut microbiota at the genus level. (F) LEfSe was performed to discriminate bacteria taxa among the different groups. Data in A and D are shown as mean ± SD and was assessed by the Kruskal–Wallis test, $n = 6$. $^{*}P < 0.05$, $^{**}P < 0.01$ and $^{***}P < 0.001$ indicated significant differences compared to the Abx group.

with the risk of pathogenic substances crossing the intercellular spaces. Although the *Ocln* gene was not affected by antibiotic exposure compared to the Con group, *ZO-1*, *Ocln*, and *Cldn1* gene expression was significantly elevated in the HH079 group (Fig. 3E–G). The reduction of occludin and claudin-1 protein expression in the Abx group also confirmed epithelial barrier impairment caused by early-life antibiotic exposure (Fig. 3H and I). The *B. breve* HH079 supplementation significantly increased colonic OCLN and CLDN1 protein expression, which might be attributed to the promoted protective colonic mucus induced by *B. breve* HH079 administration.

B. breve HH079 maintains the balance of M1/M2 macrophages and alleviates intestinal inflammation in early-life antibiotic-exposed pups

Inflammatory cytokine markers were assessed in the serum and colon tissue collected from pups at antibiotic exposure end points. Early-life antibiotic treatment significantly increased the serum TNF-α, IL-1β and LBP production and decreased anti-inflammatory cytokine IL-10 compared to the Con group (Fig. 4A–D). Interestingly, pro-inflammatory cytokines induced by antibiotic exposure in the pup serum were significantly inhibited in the HH079 group. At the colonic mRNA level, early-life antibiotic exposure stimulated *Tnf-α* and *IL-1β* gene expression and suppressed the *IL-10* gene expression compared to the Con group (Fig. 4E). *B. breve* HH079 showed anti-inflammatory properties by a significant reduction in *IL-1β* and an increment of the *IL-10* mRNA expression.

To evaluate the effect of *B. breve* HH079 administration on colonic immune development following early-life antibiotic exposure, we measured the colonic macrophage expression. Our flow cytometric analysis results showed that early-life antibiotic exposure significantly increased the percentage of colonic total macrophages ($F4/80^{+}CD11b^{+}$), whereas *B. breve* HH079 supplementation significantly decreased the total macrophage number compared to the Abx group (Fig. 4F and G). Macrophages in the lamina propria of the colon respond rapidly to stimuli by polarizing into two functionally distinct types: M1-like for pro-inflammatory responses and M2-like for anti-inflammatory responses.[35] Early-life antibiotic exposure only promoted the *Cd86* (M1 macrophage marker) gene

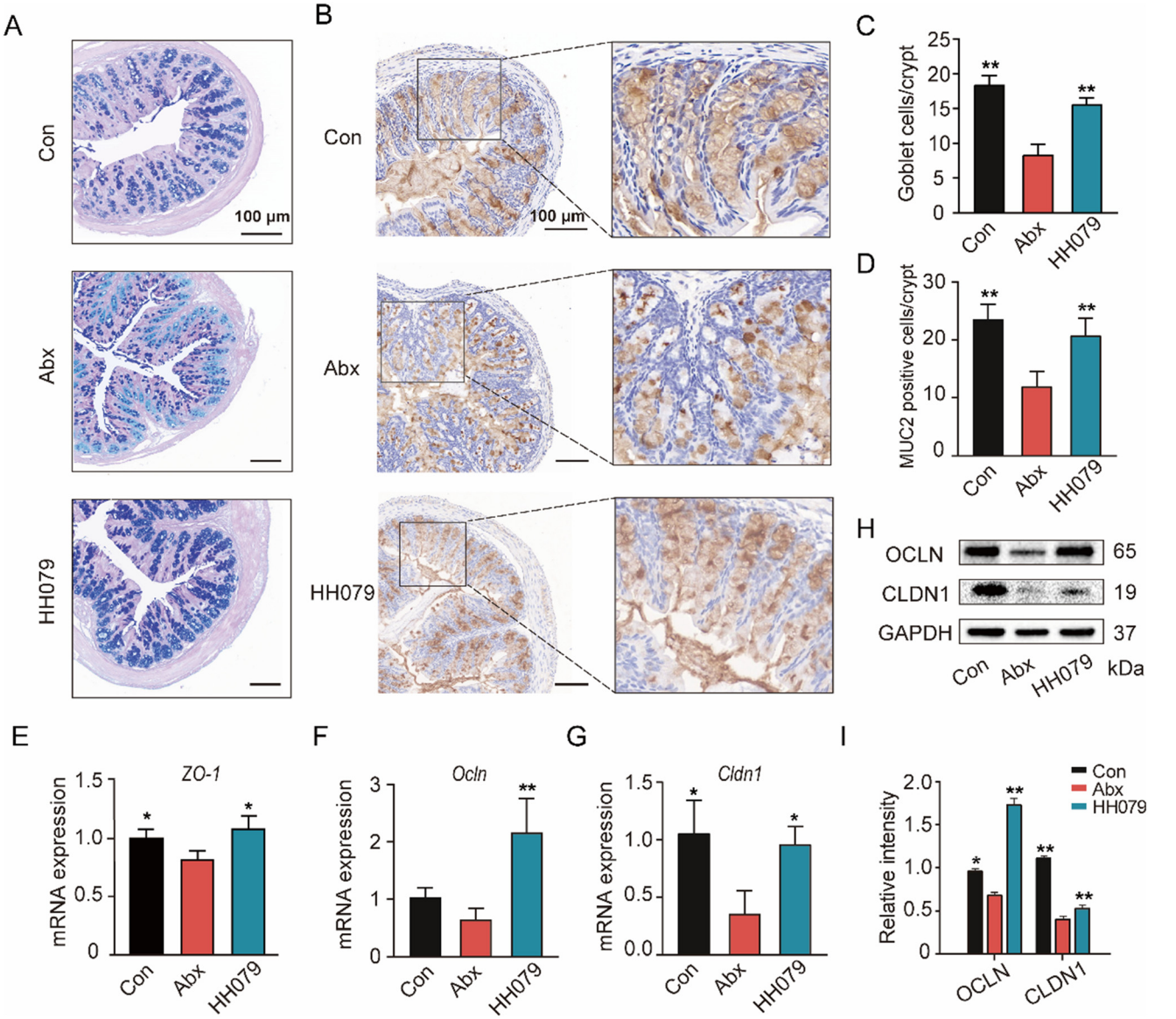

Fig. 3 *B. breve* HH079 repairs antibiotic damage to the intestinal barrier in early-life antibiotic-exposed pups. (A and C) Representative images obtained and quantification of colon goblet cells by AB/PAS staining. (B and D) Determination and quantification of the protein MUC2 in the mouse colon by immunohistochemistry (brown indicated positive target protein, $n = 3$). (E–G) Relative expression of TJ mRNA (*ZO-1*, *Ocld* and *Cldn1*, $n = 4$) in the colon. (H and I) The expression of OCLN and CLDN1 proteins was determined by WB. $^{*}P < 0.05$ and $^{**}P < 0.01$ indicated significant differences compared to the Abx group.

expression in the pup colon compared to the Con group, while *B. breve* HH079 administration reversed the increase of the *Cd86* gene and promoted the *Cd206* (M2 macrophage marker) gene expression compared with the Abx group (Fig. 4H). Additionally, the colonic iNOS protein expression was significantly lower and the Arg1 protein expression was significantly increased in the HH079 group when compared with the antibiotic-challenged pups (Fig. 4I). These results suggested that the *B. breve* HH079 supplementation could modulate pro-inflammatory cytokine responses and colonic M1 macrophage polarization triggered by early-life antibiotic exposure.

B. breve HH079 modulates colonic functional genes and NF-κB signaling pathways of early-life antibiotic-exposed pups

The RNA sequencing-based transcriptome was used to investigate the effects of *B. breve* HH079 on the gene expression in the pup colon induced by early-life antibiotic exposure. Principal component analysis (PCA) revealed an obvious shift of the colon transcriptome profiles across the different groups, suggesting that early-life intestinal epithelial damage affected the gene expression in the pup colon (Fig. 5A). We further identified differentially expressed genes (DEGs), and found that early-life antibiotic exposure resulted in a significant upre-

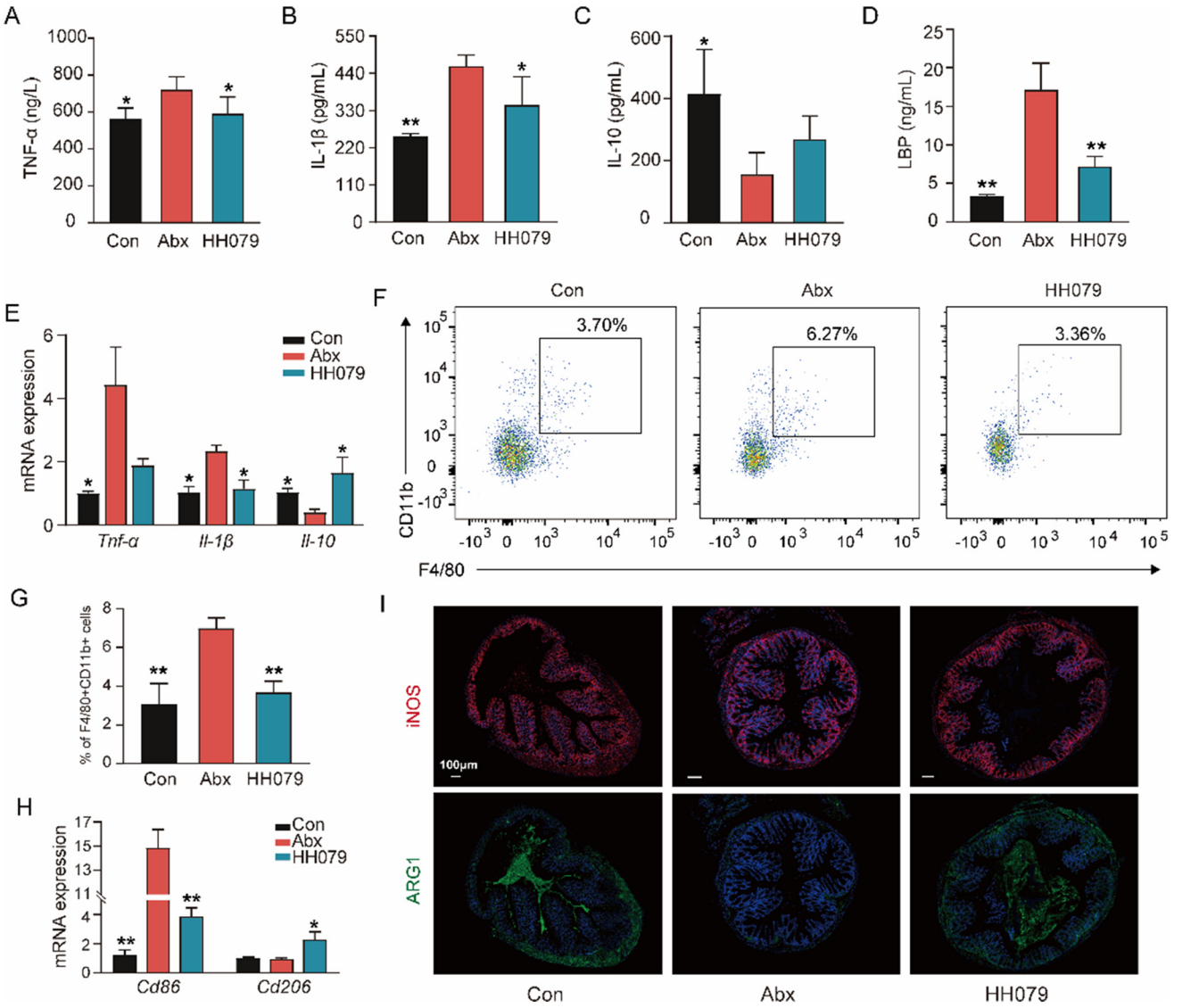

Fig. 4 *B. breve* HH079 protects colon immune balance in early-life antibiotic-exposed pups. (A and B) Concentrations of the pro-inflammatory cytokines TNF-α and IL-1β and (C) concentrations of the anti-inflammatory cytokine IL-10 in the serum. (D) LBP concentration in the serum. (E) Relative mRNA expression of *Tnf-α, IL-1β* and *IL-10* in the colon. (F and G) Representative flow cytometry plots and the prevalence of macrophages ($F4/80^{+}CD11b^{+}$). (H) The mRNA expression of *Cd86* and *Cd206* in the colon. (I) Immunofluorescence staining of iNOS (red) and Arg1 (green) to label the macrophage subtypes in the colon (n = 3 per group). $^{*}P < 0.05$ and $^{**}P < 0.01$ indicated significant differences compared to the Abx group.

gulation of 688 genes and significant downregulation of 1177 genes in the colons of pups (Fig. 5B and C). Compared to the Abx group, the HH079 group had 605 genes up-regulated and 545 genes down-regulated (Fig. 5B–D), indicating that the *B. breve* HH079 supplementation regulated the expression of genes in early-life antibiotic-exposed pups. For example, *B. breve* HH079 significantly reversed the expression of inflammatory mediators and antimicrobial defense genes that were inhibited by early-life antibiotic exposure, including *Fut9*, *Nxpe2*, *Il22ra2*, *Cd53*, *Reg3β*, and *Retnlb* (Fig. 5E and F). The sIgA response is the first line of defense for immune homeostasis, and regulated by the gut microbiota.[36] The colonic *Igha* gene expression was significantly increased in the HH079 group, which was associated with the fact that *B. breve* HH079 modulates the gut microbiota of pups severely disrupted by the antibiotic treatment (Fig. 5E). Moreover, early-life antibiotic exposure caused the up-regulation of colonic M1 macrophage marker genes such as *Il6ra*, *Nos1*, *Ccl20*, *Cxcl12*, and *Il1r1* of pups (Fig. 5G). The transcriptome results showed that *B. breve* HH079 administration reversed the M1 macrophage-related pro-inflammatory gene expression, while significantly promoting the M2 macrophage-related gene expression (Fig. 5H).

The KEGG analysis of the genes with DEG expression in *B. breve* HH079-treated early-life antibiotic exposure pups demonstrated that transcriptome changes were primarily associated with the ECM–receptor interaction, viral protein interaction with the cytokine and the cytokine receptor, IL-17

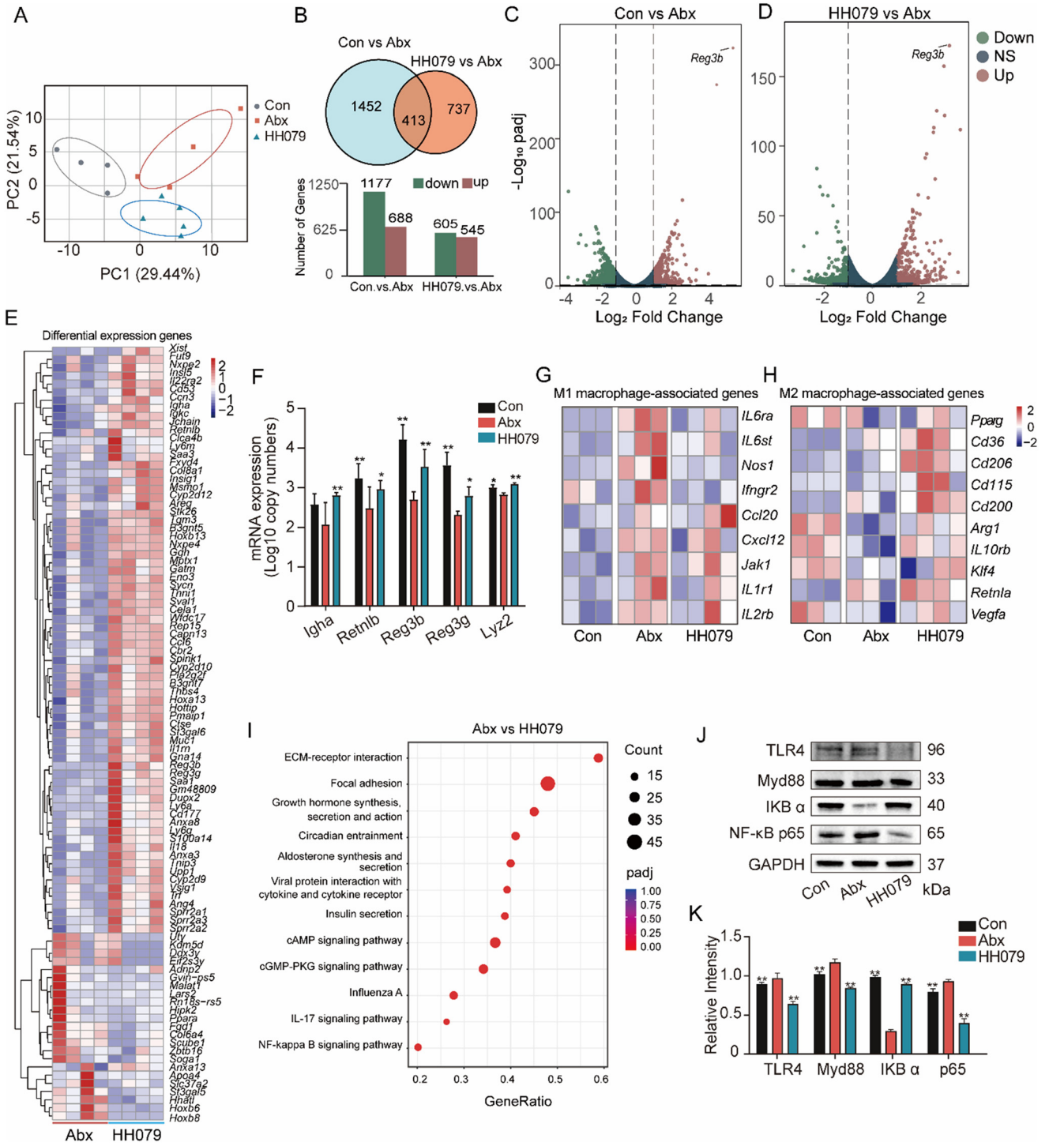

Fig. 5 *B. breve* HH079 modulates functional genes and inflammatory signaling pathways in the colons of early-life antibiotic-exposed pups. (A) PCA analysis of the gene expression. (B) Venn diagram showing the number of unique or shared genes between the DEGs of Con Abx and HH079 Abx groups. (C and D) Differential gene expression by RNA sequencing in the different treatment groups visualized using volcano plots. Different quadrants represent significantly different genes that are upregulated (red) or downregulated (green). (E) The top 100 differentially expressed genes (FC > 1 and FDR < 0.05) between the HH079 group and the Abx group. (F) Expression of genes involved in antibacterial defense. (G and H) Expression of M1 and M2 macrophage-associated marker genes. (I) Significantly enriched pathways for differentially expressed genes were identified using KEGG. (J and K) Expression and quantification of proteins in the NF-κB signaling pathway determined by WB relative to the GAPDH. Data in the bar plot are shown as mean ± SD and were assessed by the Kruskal–Wallis test. *$P < 0.05$ and **$P < 0.01$ indicated significant differences compared to the Abx group.

signaling pathway, and nuclear factor kappa-B (NF-κB) signaling pathway (Fig. 5I). In contrast to the observations in *B. breve* HH079-treated mice, early-life antibiotic exposure significantly increased the colonic protein levels of TLR4, Myd88, and NF-κB p65 of the pups, as assessed though WB analysis (Fig. 5J and K). These results suggested that *B. breve* HH079 is involved in modulating colonic barrier damage triggered by early-life antibiotic exposure in pups *via* inhibiting the NF-κB signaling pathway.

B. breve HH079 increases acetate content in early-life antibiotic-exposed pups

Early-life antibiotic exposure significantly reduced the intestinal acetate levels, which was determined by measuring the SCFA concentrations in the pup colonic contents. The acetate concentration was significantly increased in the HH079 group compared to the Abx pups (Fig. 6A). Acetate as a signaling molecule could regulate host homeostasis through G-protein-coupled receptors (GPCRs) expressed in the intestinal epithelium, mainly GPR43. Early-life antibiotic exposure significantly reduced the colon GPR43 expression in pups compared to the Con group, while *B. breve* HH079 administration significantly reversed the GPR43 expression ($p < 0.05$, Fig. 6B and C).

We performed Pearson's correlation analysis of gut microbiota and the acetate data, inflammatory cytokines and qPCR results of colon macrophage and epithelial barrier function markers. As shown in Fig. 6D, *Bacteroides* and *Bifidobacterium* were positively correlated with acetate, the M2 macrophage markers (*Cd206* and IL-10) and the intestinal barrier function gene (*Ocln*, *Cldn* and *ZO-1*), and were negatively correlated with the M1 macrophage markers (*Cd86*, TNF-α, LBP and IL-1β). Meanwhile, *Morganella*, *Pseudomonas*, *Enterococcus*, and *Paenibacillus* were negatively correlated with the M2 macrophage markers (*Cd206* and IL-10) and acetate. These

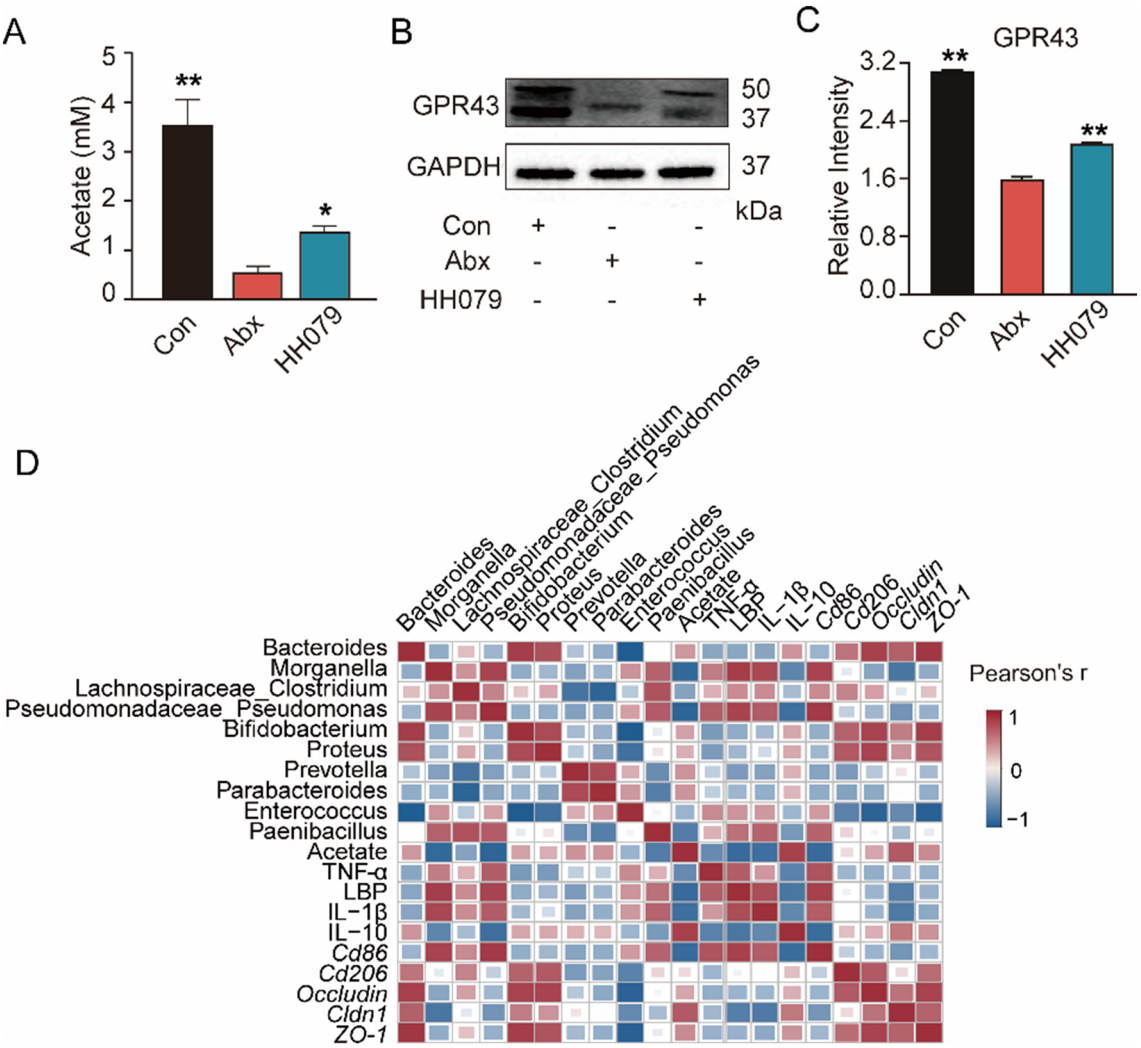

Fig. 6 Pearson's correlation analysis between the microbiome and host factor (barrier function, immune marker expression, and acetate from the colonic contents) data. (A) Concentration of acetate in the pup colonic contents. (B) Expression of GPR43 in the colon. (C) Relative intensity analysis of GPR43 in the colon. Relative protein levels were normalized to the control GAPDH. (D) Heat map illustrating the correlation between top 10 genera and host factors. *$P < 0.05$ and **$P < 0.01$ indicated significant differences compared to the Abx group.

results provide strong evidence that the *B. breve* HH079 supplementation significantly enriched the acetate-producing bacteria *Bacteroides* and *Bifidobacterium* during early-life antibiotic exposure, which positively impacts regulating colon M2 macrophage polarization and gut barrier integrity.

Discussion

Early life is a window for host gut microbiota development, which can be challenged by antibiotic exposure, increasing the risk of infections and other diseases.[37–39] In our study, dams were given antibiotic water continuously during lactation, and pups received antibiotic exposure by ingesting maternal breast milk from postnatal day 1 to day 21. We observed that early-life antibiotic exposure promoted the enrichment of Proteobacteria, including *Morganella*, *Pseudomonas*, *Enterococcus* and *Paenibacillus* (Fig. 2C–F), which are conditional pathogens that could cause various infections.[32] It was also observed that early-life antibiotic exposure resulted in weight loss and shortened colon length in pups compared with non-exposed mice (Fig. 1C and E), suggesting that negative impact of early-life antibiotic exposure on development is related to gut microbiota changes.[40] Consistent with the previous finding, antibiotic treatments blocked the increased antimicrobial gene expression in the small intestine of neonatal mice.[41] We observed a reduced expression of *Reg3β* in the colons of pups (Fig. 5F), which makes it easier for pathogenic Gram-negative bacteria to translocate into the internal mucus layer, increasing the risk of intestinal inflammation.[42] We observed increased intestinal permeability in early-life antibiotic-exposed mice, including decreased tight junction proteins and goblet cells (Fig. 3A and H). This is attributed to antibiotics destroying symbiotic bacteria in the colon, and the enrichment of drug-resistant bacteria (*Morganella* and *Pseudomonas*) and their derivatives such as LPS would affect the intestinal barrier integrity.[43] Early-life antibiotic exposure promoted the expression of M1 macrophage markers in the mouse colon (Fig. 4F and I and 5G), likely associated with the increased level of LPS.[44] Consistent with our report, Kim *et al.*[45] reported that antibiotic treatment leads to a dramatic decrease in colonic CD206$^+$ macrophages during postnatal days 14–17, affecting intestinal stem cell differentiation and causing intestinal damage in pups. Furthermore, the increased LPS in antibiotic-exposed pups activated the colonic TLR4/NF-κB pathway, promoting IL-1β and TNF-α contents and causing intestinal barrier damage (Fig. 4A–D and 5J).

We further investigated the role of *B. breve* HH079 in alleviating colon dysbiosis triggered by early-life antibiotics. *B. breve* HH079 supplementation rescued weight loss and colon shortening in pups caused by early-life antibiotic exposure (Fig. 1C–E). Interestingly, *B. breve* HH079 administration promoted the enrichment of acetate-producing members *Bacteroides* and *Bifidobacterium* (Fig. 2E and F). The increased abundance of *Bacteroides* and *Bifidobacterium* resulted in an elevated acetate concentration in the colonic contents of pups (Fig. 6A),[46] creating a non-permissive environment for the growth of pathogenic bacteria.[47] The modulation of innate defense genes (*Igha*, *Reg3β*, and *Retnlb*, Fig. 5F) by *B. breve* HH079 supplementation also supports the trend toward restoration of the gut microbiota. In fact, *B. breve* HH079 administration reversed the increase in gut penetrability (Fig. 3E–H) and promoted the colonic acidic

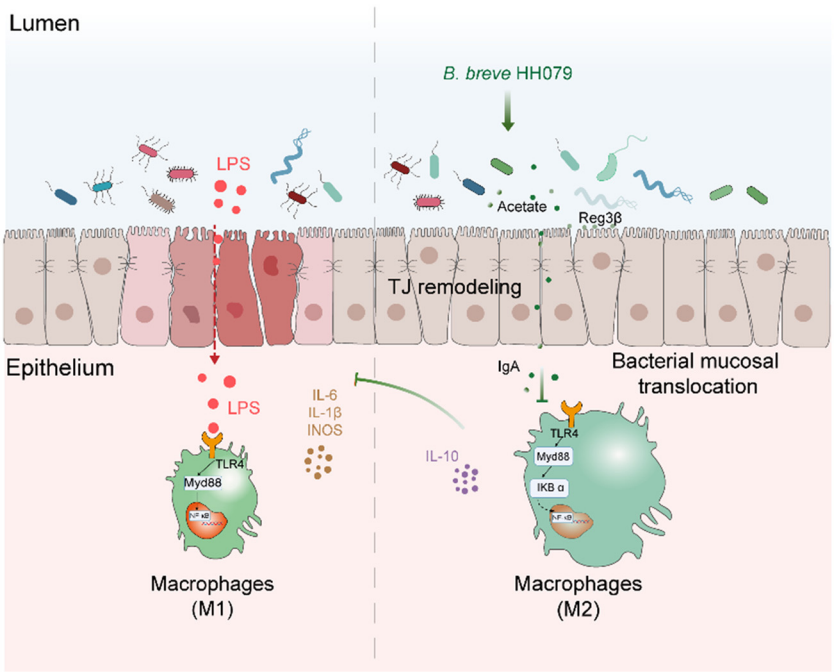

Fig. 7 A potential mechanism related to the regulation of intestinal dysregulation of *B. breve* HH079 during early-life antibiotic exposure.

mucin-filled GC number (Fig. 3A and B) of the pups, likely benefiting from the promotion of *Bifidobacteria* which colonize the intestinal mucus layer.[48] The disruption of the gut microbiota composition by a high relative abundance of harmful bacteria increased intestinal permeability, allowing LPS to penetrate the lamina propria of the pup colon. We observed that *B. breve* HH079 supplementation reduced pro-inflammatory mediators levels, such as LPS, and increased the anti-inflammatory cytokine IL-10 (Fig. 4D and E). The potential explanation could be the proliferation of *Bifidobacteria* within the gut niches in early life, which alleviates the leakage of the intestinal barrier and thus decreases the inflammatory responses.[49] *B. breve* HH079 supplementation protected the intestinal epithelial barrier integrity during early-life antibiotic exposure, and was related to the inhibition of the TLR4/NF-κB pathway (Fig. 5J and K). Mechanistically, acetate inhibits NF-κB signaling and downregulates pro-inflammatory cytokines *via* the GPR43 receptor (Fig. 6B) in pups, which were reported previously.[50,51] Moreover, the NF-κB signaling pathway has been shown to exert a strong regulatory function in mediating macrophage polarization.[52] Macrophages being polarized from the M1 phenotype to M2 phenotype after *B. breve* HH079 supplementation was related to increased acetate concentration. Our results suggested that *B. breve* HH079 supplementation could activate M2 macrophage polarization by inhibiting the TLR4/NF-κB pathway, further maintaining intestinal immune homeostasis and intestinal barrier function (Fig. 7).

Conclusion

In conclusion, the effect of *B. breve* HH079 administration on gut dysbiosis in antibiotic-exposed pups was investigated. We found that *B. breve* HH079 administration mitigated the detrimental effects of early-life antibiotic exposure on colon growth in a neonatal mouse model. *B. breve* HH079 reshaped the disrupted gut microbiota by increasing *Bacteroides* and *Bifidobacterium* abundance, and decreasing *Morganella* and *Pseudomonas* abundance in antibiotic-exposed pups. *B. breve* HH079 administration increased intestine acetate concentrations and downregulated the expression of M1 macrophage markers (*Cd86*, TNF-α, LBP and IL-1β) in the offspring. Moreover, *B. breve* HH079 inhibited the TLR4/NF-κB signaling pathway, upregulated the M2 macrophage markers (*Cd206* and IL-10) and enhanced the expression of intestinal barrier function genes (*Ocln*, *Cldn* and *ZO-1*), thereby repairing intestinal epithelial barrier dysfunction and integrity damage caused by early-life antibiotic exposure. Future research would focus on the validation of the key pathways in immune cells targeted by *B. breve* HH079 and clinical intervention for intestinal dysbiosis-associated disorders of infants.

Author contributions

Zhipeng Gu: data curation, software, roles/writing – original draft, formal analysis, methodology, conceptualization, visualization, and writing – review and editing. Zerong Lu: investigation, methodology and visualization. Jian-yong Wu: supervision and validation. Zhuqing Xie: writing – review and editing. Ruibiao Hu: writing – review and editing and resources. Qiang Huang: supervision and writing – review and editing. Feitong Liu: resources, methodology, project administration, supervision, and writing – review and editing. Bin Zhang: funding acquisition, project administration, supervision, and writing – review and editing. All authors reviewed the manuscript and approved the final version.

Data availability

The datasets supporting this article have been uploaded as part of the ESI.†

Conflicts of interest

The authors have declared no competing interests.

Acknowledgements

B. Z. acknowledged the financial support from the Guangdong Basic and Applied Basic Research Foundation (2024A1515011121).

References

1 M. Dinleyici, G. K. Yildirim, O. Aydemir, T. B. Kaya, Y. Bildirici and K. B. Carman, Human milk antibiotic residue levels and their relationship with delivery mode, maternal antibiotic use and maternal dietary habits, *Eur. Rev. Med. Pharmacol. Sci.*, 2018, **22**, 6560–6566.
2 J. L. Mathew, Effect of maternal antibiotics on breast feeding infants, *Postgrad. Med. J.*, 2004, **80**, 196–200.
3 S. C. Li, M. Cao, Y. Zhou, C. Shu and Y. Wang, Ornidazole Transfer into Colostrum and Assessment of Exposure Risk for Breastfeeding Infant: A Population Pharmacokinetic Analysis, *Pharmaceutics*, 2023, **15**, 2524.
4 H. Huang, J. Jiang, X. Wang, K. Jiang and H. Cao, Exposure to prescribed medication in early life and impacts on gut microbiota and disease development, *EClinicalMedicine*, 2024, **68**, 102428.
5 M. Mubanga, C. Lundholm, B. M. D'Onofrio, M. Stratmann, A. Hedman and C. Almqvist, Association of Early Life Exposure to Antibiotics With Risk of Atopic Dermatitis in Sweden, *JAMA Netw. Open*, 2021, **4**, e215245.
6 M. O. Coker, A. G. Hoen, E. Dade, S. Lundgren, Z. Li, A. D. Wong, M. S. Zens, T. J. Palys, H. G. Morrison, M. L. Sogin, E. R. Baker, M. R. Karagas and J. C. Madan, Specific class of intrapartum antibiotics relates to maturation of the infant gut microbiota: a prospective cohort study, *BJOG*, 2020, **127**, 217–227.

7 N. A. Scott, A. Andrusaite, P. Andersen, M. Lawson, C. Alcon-Giner, C. Leclaire, S. Caim, G. Le Gall, T. Shaw, J. P. R. Connolly, A. J. Roe, H. Wessel, A. Bravo-Blas, C. A. Thomson, V. Kästele, P. Wang, D. A. Peterson, A. Bancroft, X. H. Li, R. Grencis, A. M. Mowat, L. J. Hall, M. A. Travis, S. W. F. Milling and E. R. Mann, Antibiotics induce sustained dysregulation of intestinal T cell immunity by perturbing macrophage homeostasis, *Sci. Transl. Med.*, 2018, **10**, eaao4755.

8 T. C. Borbet, M. B. Pawline, J. Li, M. L. Ho, Y. S. Yin, X. Z. Zhang, E. Novikova, K. Jackson, B. J. Mullins, V. E. Ruiz, M. J. Hines, X. S. Zhang, A. Müller, S. B. Koralov and M. J. Blaser, Disruption of the early-life microbiota alters Peyer's patch development and germinal center formation in gastrointestinal-associated lymphoid tissue, *iScience*, 2023, **26**, 106810.

9 K. Pärnänen, A. Karkman, J. Hultman, C. Lyra, J. Bengtsson-Palme, D. G. J. Larsson, S. Rautava, E. Isolauri, S. Salminen, H. Kumar, R. Satokari and M. Virta, Maternal gut and breast milk microbiota affect infant gut antibiotic resistome and mobile genetic elements, *Nat. Commun.*, 2018, **9**, 3891.

10 D. V. Patangia, G. Grimaud, C. A. O'Shea, C. A. Ryan, E. Dempsey, C. Stanton and R. P. Ross, Early life exposure of infants to benzylpenicillin and gentamicin is associated with a persistent amplification of the gut resistome, *Microbiome*, 2024, **12**, 19.

11 L. Xiao, J. Wang, J. Zheng, X. Li and F. Zhao, Deterministic transition of enterotypes shapes the infant gut microbiome at an early age, *Genome Biol.*, 2021, **22**, 243.

12 A. Horigome, K. Hisata, T. Odamaki, N. Iwabuchi, J. Z. Xiao and T. Shimizu, Colonization of Supplemented Bifidobacterium breve M-16 V in Low Birth Weight Infants and Its Effects on Their Gut Microbiota Weeks Post-administration, *Front. Microbiol.*, 2021, **12**, 610080.

13 J. E. Kim, B. Li, L. J. Fei, R. Home, D. R. Y. Lee, A. K. Loe, H. Miyake, E. Ayar, D. K. Kim, M. G. Surette, D. J. Philpott, P. Sherman, G. J. Guo, A. Pierro and T. H. Kim, Gut microbiota promotes stem cell differentiation through macrophage and mesenchymal niches in early postnatal development, *Immunity*, 2022, **55**, 2300–2317.

14 B. Sanyang, T. I. de Silva, B. Camara, N. Beloum, A. Kanteh, J. Manneh, W. A. A. D. Piters, D. Bogaert, A. K. Sesay and A. Roca, Effect of intrapartum azithromycin on gut microbiota development in early childhood: A post hoc analysis of a double-blind randomized trial, *iScience*, 2024, **27**, 110626.

15 K. Korpela, A. Salonen, O. Vepsäläinen, M. Suomalainen, C. Kolmeder, M. Varjosalo, S. Miettinen, K. Kukkonen, E. Savilahti, M. Kuitunen and W. M. de Vos, Probiotic supplementation restores normal microbiota composition and function in antibiotic-treated and in caesarean-born infants, *Microbiome*, 2018, **6**, 182.

16 S. J. Gavzy, A. Kensiski, Z. L. Lee, E. F. Mongodin, B. Ma and J. S. Bromberg, Bifidobacterium mechanisms of immune modulation and tolerance, *Gut Microbes*, 2023, **15**, 2291164.

17 A. Zablocka, D. Jakubczyk, K. Leszczynska, K. Pacyga-Prus, J. Macala and S. Górska, Studies of the Impact of the Bifidobacterium Species on Inducible Nitric Oxide Synthase Expression and Nitric Oxide Production in Murine Macrophages of the BMDM Cell Line, *Probiotics Antimicrob.*, 2023, **16**, 1012–1025.

18 C. Alba, M. Carrera, G. Alvarez-Calatayud, R. Arroyo, L. Fernández and J. M. Rodríguez, Evaluation of Safety and Beneficial Health Effects of the Human-Milk Strain Bifidobacterium breve DSM32583: An Infant Pilot Trial, *Nutrients*, 2024, **16**, 1134.

19 Y. Q. Huang, Z. R. Lu, F. T. Liu, J. Lane, J. C. Chen, X. Fu, Q. Huang, R. B. Hu and B. Zhang, Osteopontin enhances the probiotic viability of Bifidobacteria in pectin-based microencapsulation subjected to in vitro infant gastrointestinal digestion, *Food Hydrocolloids*, 2024, **149**, 109634.

20 M. A. Lynn, G. Eden, F. J. Ryan, J. Bensalem, X. M. Wang, S. J. Blake, J. M. Choo, Y. T. Chern, A. Sribnaia, J. James, S. C. Benson, L. Sandeman, J. L. Xie, S. Hassiotis, E. W. Sun, A. M. Martin, M. D. Keller, D. J. Keating, T. J. Sargeant, C. G. Proud, S. L. Wesselingh, G. B. Rogers and D. J. Lynn, The composition of the gut microbiota following early-life antibiotic exposure affects host health and longevity in later life, *Cell Rep.*, 2021, **36**, 109564.

21 H. Zheng, X. Zhang, C. Li, D. Wang, Y. Y. Shen, J. H. Lu, L. C. Zhao, X. K. Li and H. C. Gao, BCAA mediated microbiota-liver-heart crosstalk regulates diabetic cardiomyopathy via FGF21, *Microbiome*, 2024, **12**, 157.

22 Y. Pi, Y. J. Wu, X. Y. Zhang, D. D. Lu, D. D. Han, J. C. Zhao, X. J. Zheng, S. Y. Zhang, H. Ye, S. Lian, Y. Bai, Z. Y. Wang, S. Y. Tao, D. J. Ni, X. H. Zou, W. Jia, G. L. Zhang, D. F. Li and J. J. Wang, Gut microbiota-derived ursodeoxycholic acid alleviates low birth weight-induced colonic inflammation by enhancing M2 macrophage polarization, *Microbiome*, 2023, **11**, 19.

23 L. Li, J. C. Chen, Y. X. Zheng, J. Lane, R. B. Hu, J. Z. Zhu, X. Fu, Q. Huang, F. T. Liu and B. Zhang, Gastro-Intestinal Digested Bovine Milk Osteopontin Modulates Gut Barrier Biomarkers In Vitro, *Mol. Nutr. Food Res.*, 2024, **68**, 202200777.

24 Z. P. Gu, Y. J. Zhu, S. M. Jiang, G. H. Xia, C. Li, X. Y. Zhang, J. C. Zhang and X. R. Shen, Tilapia head glycolipids reduce inflammation by regulating the gut microbiota in dextran sulphate sodium-induced colitis mice, *Food Funct.*, 2020, **11**, 3245–3255.

25 B. J. Callahan, P. J. McMurdie, M. J. Rosen, A. W. Han, A. J. A. Johnson and S. P. Holmes, DADA2: High-resolution sample inference from Illumina amplicon data, *Nat. Methods*, 2016, **13**, 581–583.

26 Z. P. Gu, S. Q. Xu, Y. X. Zheng, J. A. Lane, S. Dhital, Q. Huang, R. B. Hu, F. T. Liu and B. Zhang, In vitro faecal fermentation metabolites of 2′-fucosyllactose protect against intestinal epithelial injury: Infant enterotype effects, *Int. Dairy J.*, 2024, **150**, 105860.

27 R. Cai, Y. X. Zheng, J. A. Lane, P. T. Huang, R. B. Hu, Q. Huang, F. T. Liu and B. Zhang, In Vitro Infant Fecal

Fermentation Metabolites of Osteopontin and 2′-Fucosyllactose Support Intestinal Barrier Function, *J. Agric. Food Chem.*, 2024, **73**, 1642–1655.
28 Y. Liao, G. K. Smyth and W. Shi, featureCounts: an efficient general purpose program for assigning sequence reads to genomic features, *Bioinformatics*, 2014, **30**, 923–930.
29 M. D. Robinson, D. J. McCarthy and G. K. Smyth, edgeR: a Bioconductor package for differential expression analysis of digital gene expression data, *Bioinformatics*, 2010, **26**, 139–140.
30 G. C. Yu, L. G. Wang, Y. Y. Han and Q. Y. He, clusterProfiler: an R Package for Comparing Biological Themes Among Gene Clusters, *OMICS*, 2012, **16**, 284–287.
31 M. A. Lynn, F. J. Ryan, Y. C. Tee, S. C. Benson and D. J. Lynn, Protocol to assess the impact of early-life antibiotic exposure on murine longevity, *STAR Protoc.*, 2022, **3**, 101220.
32 H. Liu, J. M. Zhu, Q. W. Hu and X. C. Rao, Morganella morganii, a non-negligent opportunistic pathogen, *Int. J. Infect. Dis.*, 2016, **50**, 10–17.
33 I. A. Kirpich, L. S. Marsano and C. J. McClain, Gut-liver axis, nutrition, and non-alcoholic fatty liver disease, *Clin. Biochem.*, 2015, **48**, 923–930.
34 C. Ternet and C. Kiel, Signaling pathways in intestinal homeostasis and colorectal cancer: KRAS at centre stage, *Cell Commun. Signaling*, 2021, **19**, 31.
35 C. Li, M. M. Xu, K. P. Wang, A. J. Adler, A. T. Vella and B. Y. Zhou, Macrophage polarization and meta-inflammation, *Transl. Res.*, 2018, **191**, 29–44.
36 A. J. Macpherson, Y. Köller and K. D. Mccoy, The bilateral responsiveness between intestinal microbes and IgA, *Trends Immunol.*, 2015, **36**, 460–470.
37 Y. Shao, S. C. Forster, E. Tsaliki, K. Vervier, A. Strang, N. Simpson, N. Kumar, M. D. Stares, A. Rodger, P. Brocklehurst, N. Field and T. D. Lawley, Stunted microbiota and opportunistic pathogen colonization in caesarean-section birth, *Nature*, 2019, **574**, 117–121.
38 J. Stevens, S. Steinmeyer, M. Bonfield, L. Peterson, T. Wang, J. Gray, I. Lewkowich, Y. Xu, Y. N. Du, M. Z. Guo, J. L. Wynn, W. Zacharias, N. Salomonis, L. Miller, C. Chougnet, D. H. O'Connor and H. Deshmukh, The balance between protective and pathogenic immune responses to pneumonia in the neonatal lung is enforced by gut microbiota, *Sci. Transl. Med.*, 2022, **14**, eabl3981.
39 L. Hoskin-Parr, A. Teyhan, A. Blocker and A. J. W. Henderson, Antibiotic exposure in the first two years of life and development of asthma and other allergic diseases by 7.5 years: A dose-dependent relationship, *Pediatr. Allergy Immunol.*, 2013, **24**, 762–771.
40 P. Tian, W. Yang, X. Guo, T. Wang, S. Tan, R. Sun, R. Xiao, Y. Wang, D. Jiao, Y. Xu, Y. Wei, Z. Wu, C. Li, L. Gao, C. Ma and X. Liang, Early life gut microbiota sustains liver-resident natural killer cells maturation via the butyrate-IL-18 axis, *Nat. Commun.*, 2023, **14**, 1710.
41 T. M. Garcia, M. van Roest, J. L. M. Vermeulen, S. Meisner, J. Koster, M. E. Wildenberg, R. M. van Elburg, V. Muncan and I. B. Renes, Altered Gut Structure and Anti-Bacterial Defense in Adult Mice Treated with Antibiotics during Early Life, *Antibiotics*, 2022, **11**, 267.
42 R. Shindo, T. Katagiri, S. Komazawa-Sakon, M. Ohmuraya, W. Takeda, Y. Nakagawa, N. Nakagata, T. Sakuma, T. Yamamoto, C. Nishiyama, T. Nishina, S. Yamazaki, H. Kameda and H. Nakano, Regenerating islet-derived protein (Reg)3β plays a crucial role in attenuation of ileitis and colitis in mice, *Biochem. Biophys. Rep.*, 2020, **21**, 100738.
43 V. Navalón-Monllor, L. Soriano-Romaní, M. Silva, M. C. L. de las Hazas, N. Hernando-Quintana, T. S. Diéguez, P. M. Esteve and J. A. Nieto, Microbiota dysbiosis caused by dietetic patterns as a promoter of Alzheimer's disease through metabolic syndrome mechanisms, *Food Funct.*, 2023, **14**, 7317–7334.
44 X. Zhou, W. Y. Li, S. Wang, P. L. Zhang, Q. Wang, J. Xiao, C. Zhang, X. Zheng, X. Y. Xu, S. J. Xue, L. J. Hui, H. B. Ji, B. Wei and H. Y. Wang, YAP Aggravates Inflammatory Bowel Disease by Regulating M1/M2 Macrophage Polarization and Gut Microbial Homeostasis, *Cell Rep.*, 2019, **27**, 1176–1189.
45 J. E. Kim, B. Li, L. J. Fei, R. Horne, D. R. Y. Lee, A. K. H. Loe, H. Miyake, E. Ayar, M. Gurma, D. K. Kim, M. G. Surette, D. J. Philpott, P. Sherman, G. J. Guo, A. Pierro and T. H. Kim, Gut microbiota promotes stem cell differentiation through macrophage and mesenchymal niches in early postnatal development (vol 55, pg 2300, 2022), *Immunity*, 2023, **56**, 2175–2175.
46 K. Gerasimidis, K. Bryden, X. F. Chen, E. Papachristou, A. Verney, M. Roig, R. Hansen, B. Nichols, R. Papadopoulou and A. Parrett, The impact of food additives, artificial sweeteners and domestic hygiene products on the human gut microbiome and its fibre fermentation capacity, *Eur. J. Nutr.*, 2020, **59**, 3213–3230.
47 S. Kuntz, C. Kunz, C. Borsch, E. Vazquez, R. Buck, M. Reutzel, G. P. Eckert and S. Rudloff, Metabolic Fate and Distribution of 2′-Fucosyllactose: Direct Influence on Gut Microbial Activity but not on Brain, *Mol. Nutr. Food Res.*, 2019, **63**, 1900035.
48 M. A. Engevik, B. Luk, A. L. Chang-Graham, A. Hall, B. Herrmann, W. Ruan, B. T. Endres, Z. C. Shi, K. W. Garey, J. M. Hyser and J. Versalovic, Bifidobacterium dentium Fortifies the Intestinal Mucus Layer via Autophagy and Calcium Signaling Pathways, *mBio*, 2019, **10**, e01087–19.
49 G. Alessandri, D. van Sinderen and M. Ventura, The genus bifidobacterium: from genomics to functionality of an important component of the mammalian gut microbiota running title: Bifidobacterial adaptation to and interaction with the host, *Comput. Struct. Biotechnol. J.*, 2021, **19**, 1472–1487.
50 T. F. Liu, J. Li, Y. X. Liu, N. Xiao, H. T. Suo, K. Xie, C. L. Yang and C. Wu, Short-Chain Fatty Acids Suppress Lipopolysaccharide-Induced Production of Nitric Oxide and Proinflammatory Cytokines Through Inhibition of NF-κB Pathway in RAW264.7 Cells, *Inflammation*, 2012, **35**, 1676–1684.

51 M. D. Xu, Z. Y. Jiang, C. L. Wang, N. Li, L. L. Bo, Y. P. Zha, J. J. Bian, Y. Zhang and X. M. Deng, Acetate attenuates inflammasome activation through GPR43-mediated Ca2+-dependent NLRP3 ubiquitination, *Exp. Mol. Med.*, 2019, **51**, 1–13.

52 J. S. Yu, T. Huang, Y. Zhang, X. T. Mao, L. J. Huang, Y. N. Li, T. T. Wu, J. Y. Zhong, Q. Cao, Y. Y. Li and J. Jin, Substrate-specific recognition of IKKs mediated by USP16 facilitates autoimmune inflammation, *Sci. Adv.*, 2021, **7**, eabc4009.